Zinc Complex of Cyclododecanone Thiosemicarbazone as Single Source Precursor for ZnS Nanoparticles by Polyol Method

JISHA GEORGE[1,], G. RATHIKA NATH[2,], V.S. LEKHA[1,] and K. RAJESH[1,*,]

[1]Department of Chemistry, University College, Thiruvananthapuram-695034, India
[2]Department of Chemistry, Kumbalathu Sankupillai Memorial Devaswom Board College, Sasthamcotta-690521, India

*Corresponding author: E-mail: rajesh_k_k@yahoo.com

Zn(II) complex of a newly synthesized ligand cyclododecanone thiosemicarbazone (CDDTSC) have been synthesized and characterized by UV-visible spectroscopy, photoluminescence, X-ray diffraction, scanning electron microscopy, EDX and transmission electron microscopy studies. Thermal decomposition properties of the complex also were studied. The complex was subjected to thermal decomposition in a high boiling solvent glycerol to get zinc sulphide nanoparticles. Highly crystalline, mono-dispersed and well defined ZnS nanoparticles were obtained in good quantity, even in the absence of capping agents.

Keywords: Molecular precursors, Cyclododecanone thiosemicarbazone, Thiosemicarbazone, Zinc sulphide nanoparticles.

INTRODUCTION

Zinc sulphide semiconductor nanoparticles, because of their size-dependent optic, electric and magnetic properties, have a variety of applications when compared with their bulk analogues [1-5]. Brennan *et al.* [6] introduced the single source molecular precursor (SSMP) method in 1989, which was proven to be efficient for the preparation of high quality nanocrystals with high surface area, fewer defects and better stoichiometry [7-9]. It is an efficient method for the synthesis of semiconductor nanoparticles with homogeneous distribution of metal ions at molecular level [10,11].

Because of having a direct band gap of 3.7 eV at 100 °C, zinc sulphide is a popular n-type semiconductor [12]. It is well recognized for its photoluminescence [13] and electroluminescence [14] and thus has numerous applications in fields such as solar cells, lasers, *etc*. It can be made in the form of particles as well as thin films. These nanoparticles and thin films have numerous applications, such as image sensors, ultrasonic transducers, photoconductors, light emitting diodes, *etc*.

This study is focused on the use of a newly prepared zinc complex of cyclododecanone thiosemicarbazone as a single source molecular precursor for the synthesis of corresponding nano-metal sulphides.

EXPERIMENTAL

All the chemicals used were of analytical grade, purchased from the commercial sources and used as such. Thiosemicarbazide and cyclododecanone from TCL, zinc(II) salt *viz.* $Zn(OOCCH_3)_2 \cdot 2H_2O$, from Sigma-Aldrich and glycerol was procured from Merck, India.

Synthesis of cyclododecanone thiosemicarbazone (CDDTSC): An equimolar ethanolic solution of cyclododecanone was added to a hot ethanolic solution of thiosemicarbazide with continuous stirring and then refluxed on a boiling water bath for 3 h. Cooling generated a white crystalline precipitate, which was separated by filtration, washed with ethanol and dried in a desiccator (**Scheme-I**). Yield 82%. Anal. calcd. (found) % for L-($C_{13}N_3SH_{25}$): C, 61.18 (61.14); H, 9.80 (10.01); N, 16.47 (16.40); S, 12.5 (12.30). Key IR bands: (KBr, v_{max}, cm⁻¹): 3404, 3217 (NH_2 symmetric and asymmetric), 3141 (N-H), 1592 (C=N), 1075 (N-N), 862 (C=S). ¹H NMR (500 MHz, DMSO, δ ppm): 8.647 (s, 1H, N-H), 7.242 (d, 1H, NH_2), 6.179 (s, 1H, NH_2), 2.365-2.340 (t, 1H, CH_2), 2.277-2.251 (t, 1H, CH_2), 1.709-1.565 (m, 2H, CH_2), 1.335-1.255 (t, 18H, CH_2). MS (EI, amu): 256 [M+H]⁺, 278 [M+Na]⁺.

Synthesis of Zn metal complex of CDDTSC: To a hot ethanolic solution of the ligand (CDDTSC), a 2:1 ethanolic
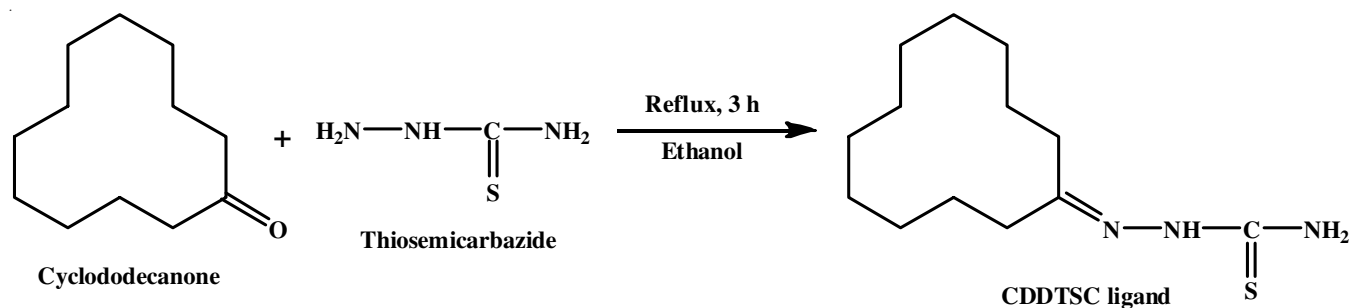
Scheme-I: Preparation of CDDTSC ligand

solution of $Zn(OOCCH_3)_2 \cdot 2H_2O$ was added and thoroughly mixed with a glass rod. The reaction mixture was then refluxed for 3 h on a water bath to complete precipitation of the corresponding zinc complex. When zinc complex cools, a white precipitate forms, which was then separated by filtration, washed with absolute ethanol and dried in a desiccator. Yield: 76%. Anal. calcd. (found) % for $C_{30}H_{56}N_6O_4S_2Zn$: C, 51.91 (54.18); H, 8.07 (8.30); N, 12.11 (14.00); S, 9.23 (11.1). IR (KBr, ν_{max}, cm^{-1}): 3415, 3302 (NH$_2$ symm. and assymm.), 3180 (N-H), 1609 (C=N), 1090 (N-N), 840 (C=S), 572, 511 (M-N), 459 (M-S).

Synthesis of nanoparticles by thermal decomposition of single source molecular precursor (SSMP) metal complex: About 15 mL of glycerol, in a boiling tube was heated over a Bunsen burner upto its boiling point (297 ºC). To the boiling solvent, added a known amount of SSMP in dispersed form in glycerol itself by placing in a sonicator bath at 75 ºC for 15 min, using a glass syringe fitted with a long needle. There was a sudden drop to ~ 70 ºC in temperature of the boiling solution. The solution was then allowed to attain the boiling point and then placed at the same condition for 20 min. The contents in the boiling tube were then transferred to a beaker containing ~ 20 mL of methanol, for sudden cooling of mixture to induce the precipitation of the corresponding metal sulphides in nano regime. After allowing the reaction mixture to cool to room temperature, the precipitated metal sulphide was separated by centrifugation. The precipitate was washed three times with methanol, transferred to a petridish and then dried again in a desiccator.

Characterization: ^{1}H NMR spectrum was recorded at 500 MHz on Bruker AMX 500 MHz FT NMR using TMS as internal standard. Mass spectrum was recorded under MS (ESI) using Thermo Scientific Extractive Orbitrap mass spectrometer.

RESULTS AND DISCUSSION

IR studies: The broad medium intensity bands observed in the IR spectrum in the range of 3400-3200 cm^{-1} and 3180-3141 cm^{-1} were assigned to the $\nu(NH_2)$ and $\nu(NHCS)$ vibrations, respectively [15,16] and these bands were found slightly affected by the metal coordination. This indicates the non-coordination of these groups in complex formation. Absence of $\nu(SH)$ band at 2570 cm^{-1} indicates that the ligand exists in thione form [17]. The band at 862 cm^{-1} assigned to the (C=S) bond also indicates the ligand's thione form [18,19]. A strong band encountered in the ligand at 1075 cm^{-1} is assigned to $\nu(N-N)$ and an increase in the frequency of this band in the spectrum of zinc complex is due to an increase in bond strengths confirming the coordination by azomethine nitrogen [17,20-23]. The band seen at 1592 cm^{-1} for free ligand, due to (C=N), was found moved towards higher wave numbers in complex formation, caused by an increase in the strength of (C=N) bond with the resulting stronger N-H in the amide group [21,23,24]. Coordination of sulphur with metal ions displaces electrons more towards the metal ions from sulphur, causing weakening of (C=S) bond shown by a decrease of vibrational frequency of C=S and hence decrease in intensity of the band in spectra of complexes [15,22,25]. The complex's IR spectra also revealed the new absorption peak at 511 cm^{-1} region corresponding to M-N bond vibrations and at 459 cm^{-1} region correspond to the metal-sulphur bond vibrations [25,26]. As a result, CDDTSC is clearly a bidentate ligand, which coordinates to the metal atoms *via* azomethine nitrogen and sulphur.

Mass studies: The electron impact mass spectrum of the ligand CDDTSC (Fig. 1) shows a strong $(m/z)^+$ peak at 278 amu corresponding to [M+Na], $([C_{13}N_3SH_{25}+Na]^+)$ and at 256 amu corresponding to [M+H]$^+$, $([C_{13}N_3SH_{25}+H]^+)$ confirming the molecular formula. Furthermore, two more peaks, one at 239 amu corresponding to the fragment after lose of NH$_2$, $[C_{13}N_2SH_{23}]^+$ and at 180 amu corresponding to the fragment after lose of –NHCSNH$_2$ group $[C_{12}H_{23}N]^+$ are seen. Intensities of peaks also give a clear idea about the stabilities of these fragments.
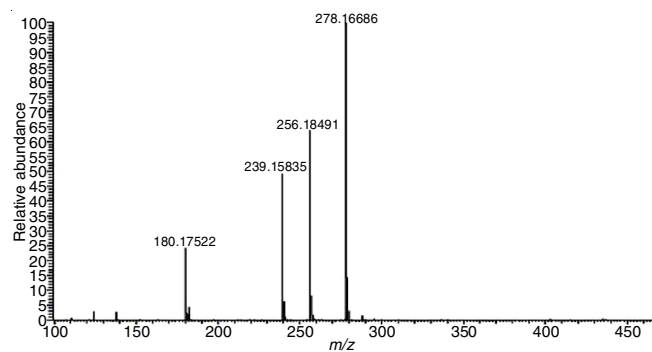

Fig. 1. MS(EI) spectrum of CDDTSC ligand

Thermal studies: Thermogravimetric analysis (TGA/DTG), gave an insight into the decomposition behaviour of the synthesized complex, under nitrogen atmosphere at the temperature range from 20 to 700 ºC. The thermal behaviour of Zn complex is depicted in Fig. 2.
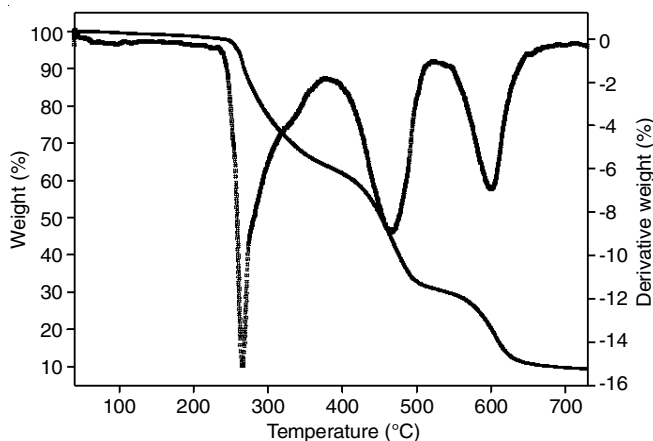
Fig. 2. TGA and DTG curves for zinc complexes

From decomposition profile of Zn(II) complex, the complex was found to decompose at 234 ºC and undergoes decomposition in three stages. The first stage is accompanied by a mass loss of (60-64%) and this weight occurred in the temperature range of 250-320 ºC. Second stage of decomposition is at (440-530 ºC), corresponding to the weight loss of 34%. The third stage was between 580-660 ºC with a slow weight loss giving ~12% of the compound as residue, which is lower than the amount of zinc sulphide calculated from the molecular formula (17%).

Characterization of nanoparticles

UV-visible spectra: The UV-vis absorption spectra of the synthesized ZnS are shown in Fig. 3. The absorption spectrum shows a blue shift in the absorption band edge when compared to bulk ZnS values (340 nm) [26]. The absorption spectrum obtained gave absorption peaks at 240 nm for ZnS. Tauc relation can be used to calculate the band gap (E_g) of synthesized nanoparticles [27]. In Tauc plot, $(\alpha h\nu)^2$ was plotted against ($h\nu$) (Fig. 4), where α is the absorption coefficient of the synthesized ZnS nanoparticles, h is the Planck's constant and ν is the frequency. The band gap for ZnS nanoparticles shows a shift from 3.65 nm to 4.08 nm, indicating the size quantization effects.
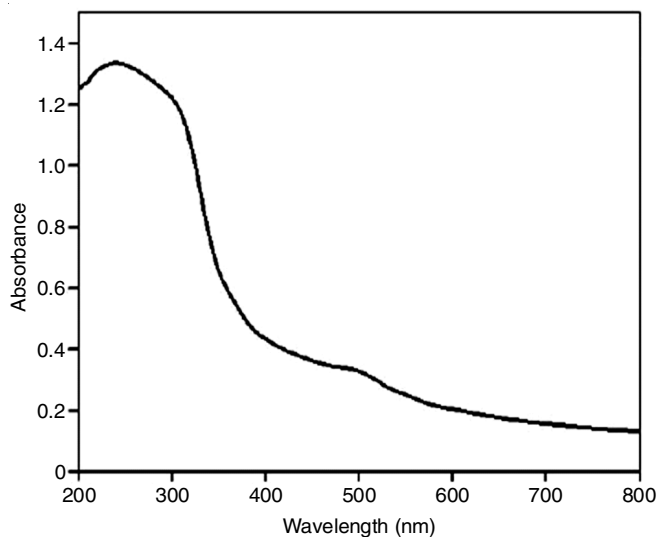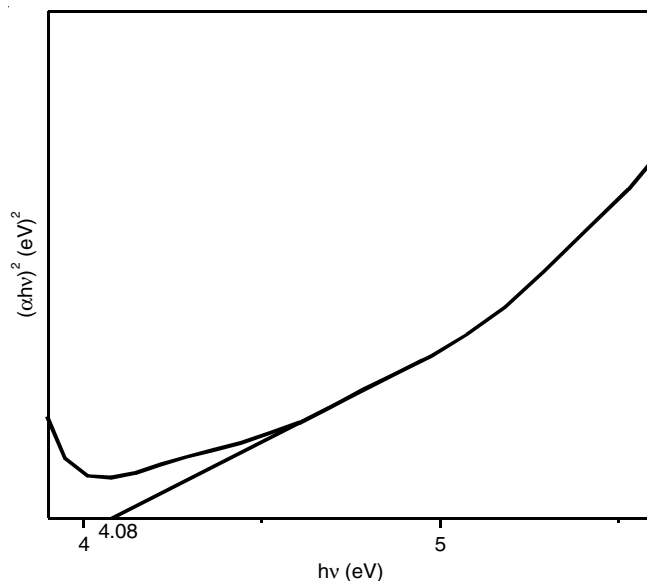

Fig. 3. UV-visible absorption spectrum of ZnS

Fig. 4. Tauc plot for ZnS

Photoluminescence studies: The photoluminescence spectrum of the synthesized nano-ZnS at room temperature was recorded using a Jasco FP 750 spectrometer at 240 nm as shown in Fig. 5. It was demonstrated that defect states like surface states, stoichiometric vacancies and interstitial lattice defects dominated nano-ZnS photoluminescence emission [28-30]. In the photoluminescent spectrum of nano-ZnS, the sharp band is centred at 468 nm, with shoulders and a broad band showing multiple asymmetric emission at higher wavelengths is also seen. A comparable result for nano-ZnS, showing a broad green emission peak is obtained in the work of Biswas *et al.* [31], which is attributed to the long range order of defects within the nanostructures.
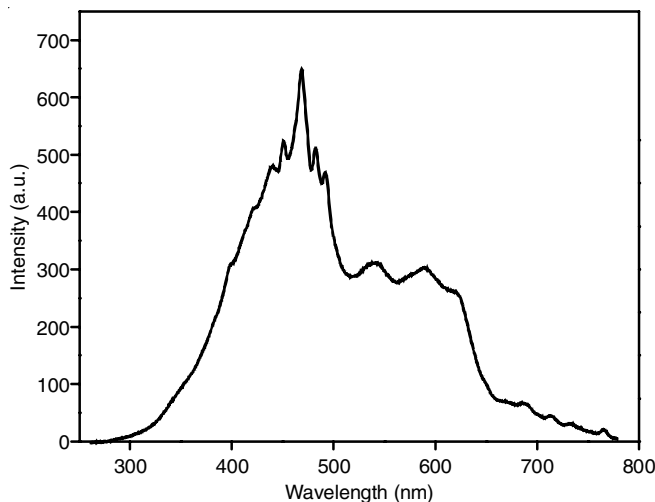

Fig. 5. Photoluminescence (PL) spectra of ZnS

X-ray diffraction (XRD) measurements: The particle size can be calculated from the X-ray diffraction peaks using the Debye Scherrer's formula:

$$D = \frac{K\lambda}{\beta \cos\theta}$$

where D = the average particle size, K = the Scherrer constant (K = 0.89), λ = the X-ray wavelength (λ = 1.5406 Å), β is the full peak width at half maximum (FWHM) and θ = the diffraction angle [32].

The XRD pattern for nano-ZnS (Fig. 6) show three main diffraction peaks indexed at (002), (110) and (112), corresponding to hexagonal ZnS planes. The obtained XRD patterns are well matched with the standard JCPDS data card No. (00-036-1450). Because of the size effect, the XRD peaks became broader and wider as the particle size decreased, indicating the presence of the nanometer regime. Using the Debye-Scherrer equation, the average particle size of the synthesized ZnS nanoparticles was calculated to be 4.44 nm. The lattice constants were calculated from XRD peaks as a = b = 3.819 Å and c = 6.261 Å, which is close to the standard values (a = b = 3.821 Å and c = 6.257 Å) reported in the JCPDS card No. (00-036-1450). Percentage crystallinity for the diffraction pattern was calculated to be 66.85.
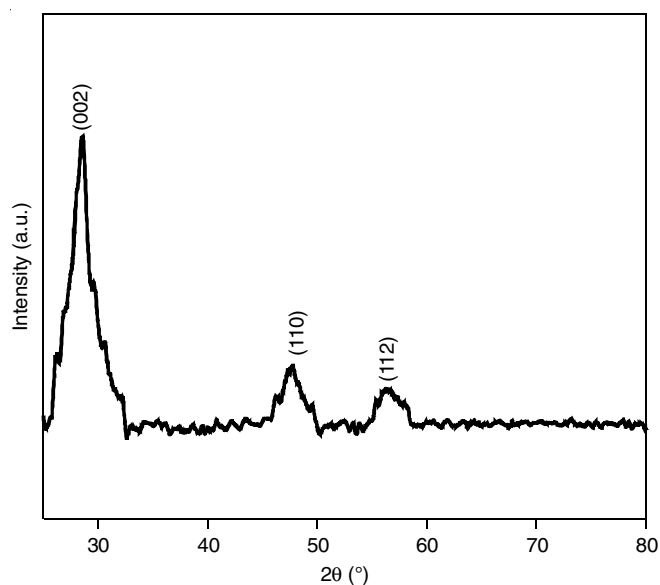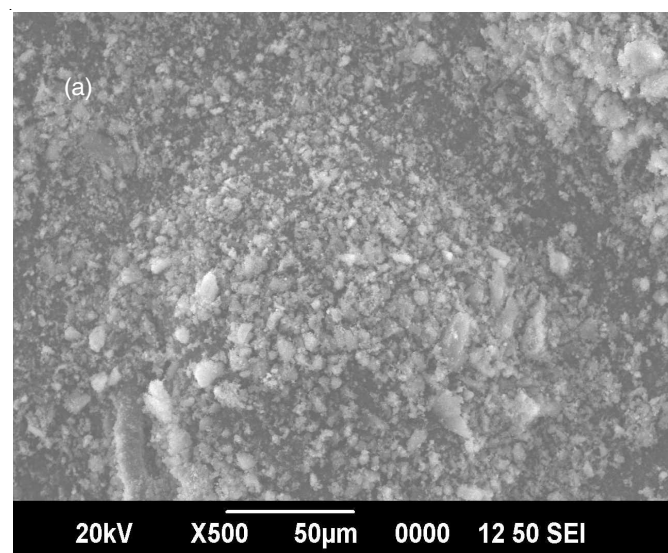

Fig. 6. XRD patterns of ZnS

SEM-EDX studies: Fig. 7a depicts FESEM images of synthesized nano-ZnS samples with spherical morphology. The crystalline nature of the particles can also be seen. The stoichiometry of the synthesized ZnS nanoparticles were estimated using EDX spectrum and is shown in Fig. 7b, which indicate that all samples were pure with zinc and sulphur only as the elementary components. For ZnS, Zn and S are present in the ratio, Zn: S as 39:61. Thus ZnS shows a metal deficiency defect in the crystal structure.

Transmission electron microscopy (TEM): TEM image of ZnS is shown in Fig. 8, which reveals a highly monodispersed and well-defined dot shaped particles with a narrow size distribution ranging from 2.64 to 6.53 nm, with a mean particle size of 4.80 nm. The selective area electron diffraction (SAED) pattern for ZnS (Fig. 8b) was found to be symmetrical and exhibits a well separated electron diffraction pattern that can be indexed to a hexagonal crystal structure. The calculated *d*-spacing values from the major rings also correspond to the *d*-spacing of the ZnS hexagonal crystalline phase. The HRTEM of ZnS nanoparticles (Fig. 8c) reveals a well-defined crystalline structure with a lattice spacing of 0.20 nm, indicating that crystal growth is occurring along the (110) direction.

Conclusion

The ligand cyclododecanone thiosemicarbazone (CDDTSC) has been synthesized successfully in good yield and characterized by the spectroscopic methods. Zinc(II) complex was also successfully synthesized and characterized by IR and thermal studies before being subjected to thermal decomposition in a high boiling solvent glycerol. The synthesized ZnS nanoparticles were obtained in a well defined, highly crystalline and monodispersed form, in comparatively good yield. Characterization of these nanoparticles were also carried out. It is clear from the studies that synthesized zinc complex of ligand CDDTSC, shows promise as efficient single source molecular precursors (SSMPs) in the nanosynthesis of the corresponding metal sulphides.
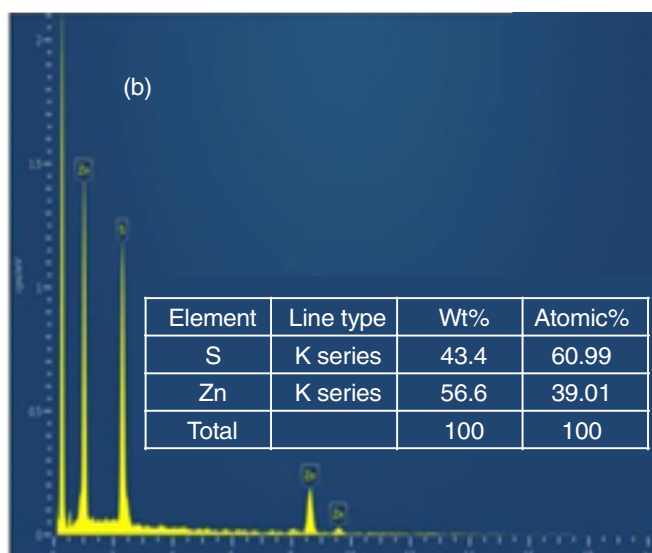

Element	Line type	Wt%	Atomic%
S	K series	43.4	60.99
Zn	K series	56.6	39.01
Total		100	100

Fig. 7. (a) SEM images and (b) EDX spectra for ZnS
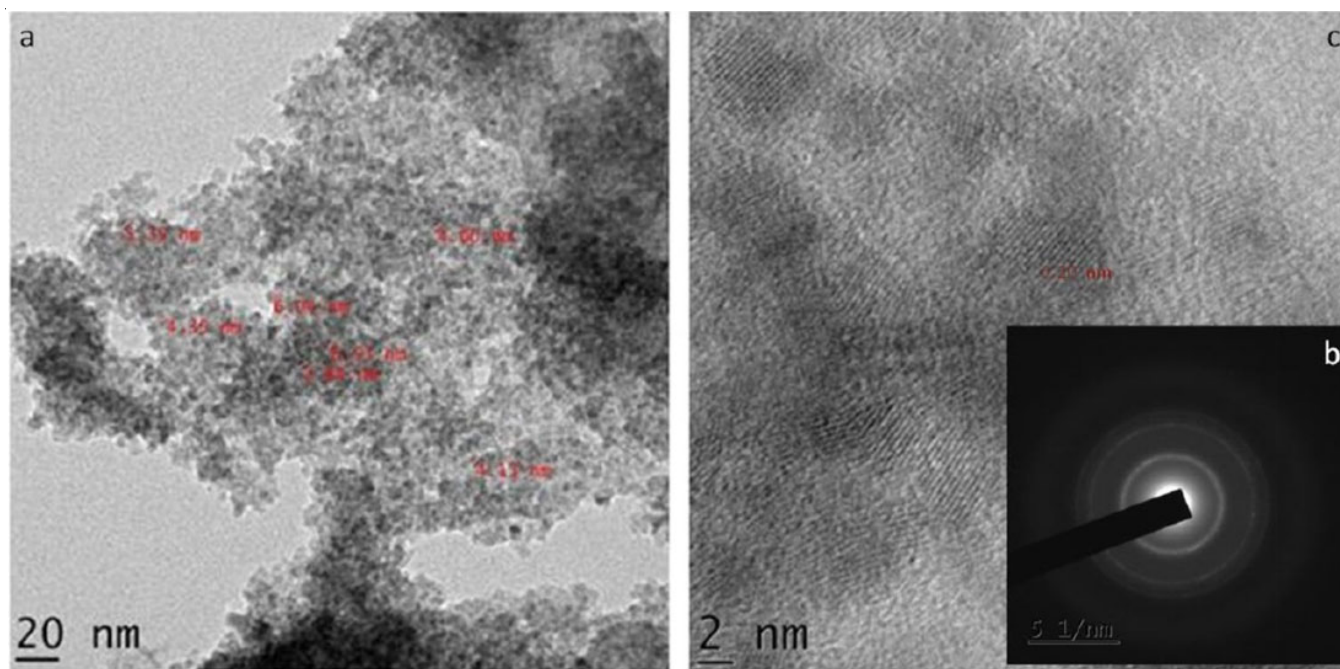
Fig. 8. (a) TEM, (b) SAED pattern and (c) HRTEM images of ZnS

CONFLICT OF INTEREST

The authors declare that there is no conflict of interests regarding the publication of this article.

REFERENCES

1. T. Trindade, P. O'Brien and N.L. Pickett, *Chem. Mater.*, **13**, 3843 (2001);
https://doi.org/10.1021/cm000843p
2. S.K. Ghosh and T. Pal, *Chem. Rev.*, **107**, 4797 (2007);
https://doi.org/10.1021/cr0680282
3. M.V. Kovalenko, L. Manna, A. Cabot, Z. Hens, D.V. Talapin, C.R. Kagan, V.I. Klimov, A.L. Rogach, P. Reiss, D.J. Milliron, P. Guyot-Sionnnest, G. Konstantatos, W.J. Parak, T. Hyeon, B.A. Korgel, C.B. Murray and W. Heiss, *ACS Nano*, **9**, 1012 (2015);
https://doi.org/10.1021/nn506223h
4. S.Z. Butler, S.M. Hollen, L. Cao, Y. Cui, J.A. Gupta, H.R. Gutiérrez, T.F. Heinz, S.S. Hong, J. Huang, A.F. Ismach, E. Johnston-Halperin, M. Kuno, V.V. Plashnitsa, R.D. Robinson, R.S. Ruoff, S. Salahuddin, J. Shan, L. Shi, M.G. Spencer, M. Terrones, W. Windl and J.E. Goldberger, *ACS Nano*, **7**, 2898 (2013);
https://doi.org/10.1021/nn400280c
5. Z. Li, J. Zhang, J. Du, T. Mu, Z. Liu, J. Chen and B. Han, *J. Appl. Polym. Sci.*, **94**, 1643 (2004);
https://doi.org/10.1002/app.21042
6. J.G. Brennan, T. Siegrist, P.J. Carroll, S.M. Stuczynski, L.E. Brus and M.L. Steigerwald, *J. Am. Chem. Soc.*, **111**, 4141 (1989);
https://doi.org/10.1021/ja00193a079
7. C.I. Pearce, R.A.D. Pattrick and D.J. Vaughan, *Rev. Mineral. Geochem.*, **61**, 127 (2006);
https://doi.org/10.2138/rmg.2006.61.3
8. M.A. Malik, M. Afzaal and P. O'Brien, *Chem. Rev.*, **110**, 4417 (2010);
https://doi.org/10.1021/cr900406f
9. G. Kedarnath, Eds.: A.K. Tyagi and R.S. Ningthoujam, Synthesis of Advanced Inorganic Materials through Molecular Precursors, Handbook on Synthesis Strategies for Advanced Materials, Indian Institute of Metals Series. Springer, Singapore (2021).
10. M. Grzelczak, J. Vermant, E.M. Furst and L.M. Liz-Marzán, *ACS Nano*, **4**, 3591 (2010);
https://doi.org/10.1021/nn100869j
11. B. Dong, T. Zhou, H. Zhang and C.Y. Li, *ACS Nano*, **7**, 5192 (2013);
https://doi.org/10.1021/nn400925q
12. K. Sooklal, B.S. Cullum, S.M. Angel and C.J. Murphy, *J. Phys. Chem.*, **100**, 4551 (1996);
https://doi.org/10.1021/jp952377a
13. C. Falcony, M. Garcia, A. Ortiz and J.C. Alonso, *J. Appl. Phys.*, **72**, 1525 (1992);
https://doi.org/10.1063/1.351720
14. W. Tang and D.C. Cameron, *Thin Solid Films*, **280**, 221 (1996);
https://doi.org/10.1016/0040-6090(95)08198-4
15. R.K. Agarwal, L. Singh and D.K. Sharma, *Bioinorg. Chem. Appl.*, **2006**, 59509 (2006);
https://doi.org/10.1155/BCA/2006/59509
16. P. Rapheal, E. Manoj and M.R.P. Kurup, *Polyhedron*, **26**, 5088 (2007);
https://doi.org/10.1016/j.poly.2007.07.028
17. A.S. Reddy, L.S. Krishna, H.K. Rashmi, P.U.M. Devi, Y. Sarala and A.V. Reddy, *J. Appl. Pharm. Sci.*, **6**, 107 (2016);
https://doi.org/10.7324/JAPS.2016.601015
18. D. Kovala-Demertzi, A. Papageorgiou, L. Papathanasis, A. Alexandratos, P. Dalezis, J.R. Miller and M.A. Demertzis, *Eur. J. Med. Chem.*, **44**, 1296 (2009);
https://doi.org/10.1016/j.ejmech.2008.08.007
19. R. Manikandan, P. Vijayan, P. Anitha, G. Prakash, P. Viswanathamurthi, R.J. Butcher, K. Velmurugan and R. Nandhakumar, *Inorg. Chim. Acta*, **421**, 80 (2014);
https://doi.org/10.1016/j.ica.2014.05.035
20. M. Joseph, V. Suni, M.R. Prathapachandra Kurup, M. Nethaji, A. Kishore and S.G. Bhat, *Polyhedron*, **23**, 3069 (2004);
https://doi.org/10.1016/j.poly.2004.09.026
21. S. Chandra and Y. Kumar, *Proc. Indian Acad. Sci. Chem. Sci.*, **92**, 249 (1983);
https://doi.org/10.1007/BF02841242
22. V.B. Rana, P.C. Jain, M.P. Swami and A.K. Srivastava, *J. Inorg. Nucl. Chem.*, **37**, 1826 (1975);
https://doi.org/10.1016/0022-1902(75)80336-8

23. M.J.M. Campbell, R. Grzeskowiak, R. Thomas and M. Goldstein, *Spectrochim. Acta A*, **32**, 553 (1976); https://doi.org/10.1016/0584-8539(76)80116-X

24. S. Chandra and M. Tyagi, *J. Serb. Chem. Soc.*, **73**, 727 (2008); https://doi.org/10.2298/JSC0807727C

25. M.S. Hossain, M.A. Mannan and M. Kudrat-E -Zahan, *Int. J. Chem. Stud.*, **4**, 17 (2020).

26. T. Xaba, B. W. Masinga and M.J. Moloto, *Digest J. Nanomater. Biostruct.*, **11**, 1231 (2016).

27. B.S. Rao, B.R. Kumar, G.V. Chalapathi, V.R. Reddy and T.S. Rao, *J. Nano- Electr. Phys.*, **3**, 620 (2011).

28. Z. Zhang, J. Wang, H. Yuan, Y. Gao, D. Liu, L. Song, Y. Xiang, X. Zhao, L. Liu, S. Luo, X. Dou, S. Mou, W. Zhou and S. Xie, *J. Phys. Chem. B*, **109**, 18352 (2005); https://doi.org/10.1021/jp052199d

29. A. Goudarzi, G.M. Aval, S.S. Park, M.C. Choi, R. Sahraei, M.H. Ullah, A. Avane and C.S. Ha, *Chem. Mater.*, **21**, 2375 (2009); https://doi.org/10.1021/cm803329w

30. Q. Wu, H. Cao, S. Zhang, X. Zhang and D. Rabinovich, *Inorg. Chem.*, **45**, 7316 (2006); https://doi.org/10.1021/ic060936u

31. S. Biswas, S. Kar, S. Santra, Y. Jompol, M. Arif and S.I. Khondaker, *J. Phys. Chem. C*, **113**, 3617 (2009); https://doi.org/10.1021/jp810177a

32. P.S. Nair, T. Radhakrishnan, N. Revaprasadu, G. Kolawole and P. O'Brien, *J. Mater. Chem.*, **12**, 2722 (2002); https://doi.org/10.1039/b202072f